International Journal of Latest Research in Humanities and Social Science (IJLRHSS)
Volume 06 - Issue 04, 2023
www.ijlrhss.com || PP. 21-30

Theoretical Analysis of Potential Selective Cyclooxygenase (Cox)-2 Inhibitors in Active Ingredients of Medicinal Plants by Molecular Docking

Rolando I. Haro Artos[1]
Ginno Andrés Alvarado Avila[2]
[2] *Departamento de Ciencias de la Vida. Universidad Estatal Amazónica (UEA). Av. C. Teniente Hugo Ortíz E45, Puyo-Ecuador*
[2]*Médico Veterinario adscrito como Docente de la Universidad Estatal Amazónica (UEA). Sede El Pangui.*

Abstract: Inflammation is a self-regulation and tissue repair mechanism when faced with an agent that can affect homeostatic processes. As the over expression of the COX-2 enzyme deregulates inflammatory processes, the inflammation can present itself as an autoimmune disease. The objective of this study was to find possible COX-2 inhibitors using 50 active principles of medicinal plants of Ecuadorian origin and a Protein Data Bank (PDB) model of the COX-2 enzyme. The technique used was Molecular Coupling in Virtual Ligand Screening through free access software. The results obtained in the study were defined by the energy expenditure values, which ranged from -0.4 to -8.6 kcal/mol, and the interactions between the amino acids of the active site and the ligand through electrical bonds. Among the best-evaluated molecules were Quercetin -8.6 kcal/mol (Rivea corymbose), Squalene -8.4 kcal/mol (Marsdenia condurango), and Tapsine -8.3 kcal/mol (Uncaria tomentosa). With this molecular Docking technique, low-cost experimentation of high scientific value can be pursued in the search for new drugs.
Keywords: Bioinformatics, Molecular docking, Arachidonic acid.

Introduction

Inflammatory processes, whose purpose is to fight injury-causing agents, are the primary defense system of the organism for tissue repair after injuries such as trauma, contusions, or even injuries of a viral nature, extreme temperatures, and ionizing radiation. Their activity lies in a cellular and microvascular biochemical cascade that promotes the removal of damaged tissue and tissue restoration (Kedika et al., 2009; Maria et al., 2018; Page & Spina, 2011).

According to Zhang et al. (2022) and Firdous and Satya (2018), failure of this immune and defense mechanism leads to under-regulated and acute inflammation, which can develop into chronic inflammation due to overexpression of inflammatory mediators involved in cell signaling and dysregulated inflammatory cell migrations. Consequently, chronic inflammation is associated with diseases with high levels of morbidity.

Thus, there are different pathways at the metabolic level through which the immune system manages to control these processes, naturally and/or induced (Zhang et al., 2022). Among the metabolic pathways, lipoxygenase (LOX) and cytochrome P450-CYP (CYP450) are involved in the synthesis of leukotrienes and prostaglandins called proinflammatory eicosanoids due to their origin in eicosapolienoic acid (Fujikura et al., 2015; Sánchez-Mendoza et al., 2003). Similarly, cyclooxygenase isoforms (COX 1/2) are essential regulators of inflammatory processes, synthesizing prostaglandins, prostanoids, and thromboxanes, through the oxidation of arachidonic acid (Bermúdez Arias, 2017; Sánchez-Mendoza et al., 2003).

Consequently, arachidonic acid (AA) and its metabolites synthesized by cyclooxygenase-2 (COX-2) or cyclooxygenase-1 (COX-1) become the molecules involved in signaling, inflammatory control, and activation of immune system cells (Sánchez-Mendoza et al., 2003). This process is carried out through the so-called arachidonic acid cascade, which releases AA from membrane phospholipids through interaction with the enzyme cytosolic phospholipase A2α (cPLA) (Kedika et al., 2009).

Through the different metabolites synthesized by the interaction between COX-1 and AA in the activation cascade, stabilization is promoted in multiple homeostatic processes in many tissues (Stachowicz, 2021). However, COX-2 is responsible for metabolizing AA in prostaglandins and thromboxanes stimulated by inflammatory processes such as tissue damage, viral infections, and tumor development through overexpression of prostaglandin E2 (PGE2), a cell metastasis-affecting enzyme (Lopez & Ballaz, 2020)

Although drug-based treatments already exist, they often present adverse effects due to undesired expression in other systems; therefore, their specificity, tolerance, and safety must be evaluated (Park et al., 2006; Zhang et al., 2022). Hence, due to their antioxidant, anticancer, and anti-inflammatory qualities, the active

principles of medicinal plants become the first agents to be studied through the regulation of multiple cell signaling pathways (Chen et al., 2022; Roskoski, 2022).

In the search for new drugs, a molecular docking tool stands out. The mapping of possible, stable interactions between the target and the molecule to be docked through a three-dimensional predictive model allows the observation of various protein-ligand interactions, protein-protein, and even genetic material between proteins or ligands. In that way, and according to the chemical and energetic characteristics of the molecule, it is possible to predict its stability and possible functioning to be incorporated a posteriori in the pharmacological kinetics at the metabolic level (Chahal et al., 2020; Jade et al., 2020).

The objective of this theoretical study is to evaluate possible COX-2 inhibitors through the interaction of medicinal plants of the Ecuadorian Sierra and Amazon regions with 50 active ingredients by using molecular docking programs, which will allow predicting the orientation, affinity, and interaction of a ligand in the specific binding site of a protein.

Materials and Methods

Selection of the protein model

The study's design was computational and comparative since it evaluated the interactions between 50 active ingredients and the COX-2 enzyme after the three-dimensional design of the active ingredients and their interaction with the COX-2 protein in a virtual environment, using the molecular docking technique.

The selection of the potential three-dimensional models was performed through the Protein Data Bank (PDB) (Danielsen et al., 2005), specifying the enzyme search origin to be COX-2 from *Homo sapiens* since the theoretical assays of the molecules are intended for possible use in humans (Roskoski, 2022).

After downloading the protein structures, the online program PROCHECK (Laskowski, R. A., MacArthur, M. W., Moss, D. S. & Thornton, 1993) was used to determine the quality of the models by stereochemical Analysis of the selected proteins. For this purpose, the comparative Analysis through the Ramachandran plot is presented in Table 1, which allows the prediction through different stereochemical parameters of the protein organization (Sobolev et al., 2020).

Table 1
Information on the three-dimensional structures of COX-2

Protein	Ligand	Resolusion	Method	Ramachandran	Referencias
5F19	2-acetamido-2-desoxi-beta-D-glucopiranose	2.04 Å	X-ray diffraction	90.7%	(Nag., Dhull, N., & Gupta, 2022)
5IKV	2-[[3-(trifluoromethyl) phenyl]amino] benzoic acid	2.51 Å	X-ray diffraction	89.4%	
5IKT	2-[(3-chloro-2-methylphenyl)amino]benzoic acid	2.45 Å	X-ray diffraction	89.5%	
5IKR	2-[(2,3-dimethylphenyl)amino]benzoic acid	2.34 Å	X-ray diffraction	90.0%	(Egwolf, B., & Gumawid, 2020)
5IKQ[a]	2-[(2,6-dichloro-3-methyl-phenyl)amino]benzoic acid	2.41 Å	X-ray diffraction	90.2%	
5KIR	Rofecoxib	2.70 Å	X-ray diffraction	88.3%	(Nag., Dhull, N., & Gupta, 2022)

5F1A	2-acetamido-2-deoxy-beta-D-glucopyranose	2.38 Å	X-ray diffraction	89.5%	(Egwolf, B., & Gumawid, 2020)

Note: The resolution values obtained in the PDB in combination with the Ramachandran percentage -which must be greater than 90%- allows the selection of the best protein model. A In this case, the 5IKQ model was selected since its resolution is high and its Ramachandran percentage is acceptable.

Digitization of active principles

The digitization was performed using bibliographic information of the active principles of plants with pharmacological uses presented in Table 2. In the process of constructing the structural models of the active principles, the chemical molecule database PubChem (Chen B, Wild D, 2009) was used to obtain the canonical SMILES of each molecule in order to structure them in a three-dimensional plane with the chemical molecule drawing software Chemsketch (Ihlenfeldt W, Bolton E, 2009).

The structural design of each molecule was downloaded in. mol format, which contains the description of the chemical structure of each compound. Subsequently, the generated .mol file was uploaded to the molecular modeling program Vega ZZ version 3.2.2.20 (Pedretti, A., & Vistoli, 2006) in order to optimize the geometry, the minimization energy, the fixing of the atomic charges, the atomic charge attribution, the adjustment of the three-dimensional coordinates, and the subsequent download in .pdb format. This format describes the complete characteristics of a three-dimensional molecule based on the Protein Data Bank (Boltzmann et al., 2013).

Finally, the .pdf file of each molecule was uploaded to Auto DockT ools software (Morris, G., Huey, R., Lindstrom, G., Sanner, M., Belew, R., Goodsell, D., & Olson, 2009) and was later modified into a .pdbqt format, which is the interaction format for the Docking process.

Table 2
List of Active Ingredients with Potential Anti-inflammatory Potential Present in Plants from Ecuador

Scientific Name	Active Principle
Arenaria jamesoniana Rohrb.	Arenarin A
	1-(7-Methoxy-9H-pyrido[3,4-b]indol-1-yl)ethan-1-one
Annona squamosa L.	Bullatacin
	Murisolin
	Squamocin
Agave americana L.	Aloe emodin
Bryophyllum pinnatum (Lam.) Oken	Bryophyllin A
	Bryophyllin B
Banisteriopsis caapi (Spruce ex Griseb.) C.V. Morton	N,N-Dimethyltryptamine
Casearia sylvestris Sw. Leaves	Casearin L
	Casearin O
	Casearvestrin A
	Casearvestrin B
	Casearvestrin C
Cinchona officinalis L	Chloroquine
Croton lechleri Mull. Arg Sap Bark Leaves	3',4-O-Dimethylcedrusin
	4,5-Dihydroblumenol A
	4-O-Methylcedrusin
	Catechin
	Epigallocatechin
	Epigallocatechin-4-8
	Procyanidin B1
Licania intrapetiolaris Spruce ex Hook. f.	Cucurbitacin B

	Intrapetacin A
Marsdenia condurango Rchb. f. Bark	1-Caffeoylquinic acid
	4-Coumarate
	4-hydroxy-3-methoxybenzaldehyde
	4-Hydroxycinnamic acid
	β-sitosterol
	Cichoriin
	Coumarin
	Saponarin
Minquartia guianensis Aubl.	Erythrodiol
	Minquartynoic acid
	Oleanolic acid
	Squalene
	Taraxerol
Monnina obtusifolia H.B.K. Aerial parts	1,3,6-Trihydroxy-2,5-dimethoxyxanthone
Prestonia mollis Kunth	Condurango glycoside A
	Tetrahydroharmine
Psychotria viridis Ruiz & Pav.	3,4-Methylenedioxymethamphetamine
	18,19-Dihydroangustine
Rivea corymbose (L.) Hallier f.	Psilocybine
	Quercetin
	Quinine
Senna multiglandulosa (Jacq.) H.S. Irwin & Barneby	Floribundone
	Physcion
Uncaria tomentosa (Will.) DC	Isomitraphylline
	Isopteropodine
	Tapsine
	Uncarine

Source: Bailon-Moscoso et al., 2015

Molecular Docking

The previously selected protein structure of COX-2 was prepared in order to extract all water molecules and protein chains that are not of interest to the study.

Subsequently, using a .pdb format, the position of the ligand was located to remove it from the active site where the interaction between the active principles and the 5IKQ protein of COX-2 took place. Purification was performed to optimize the protein and reduce the processing time (Figure 1).

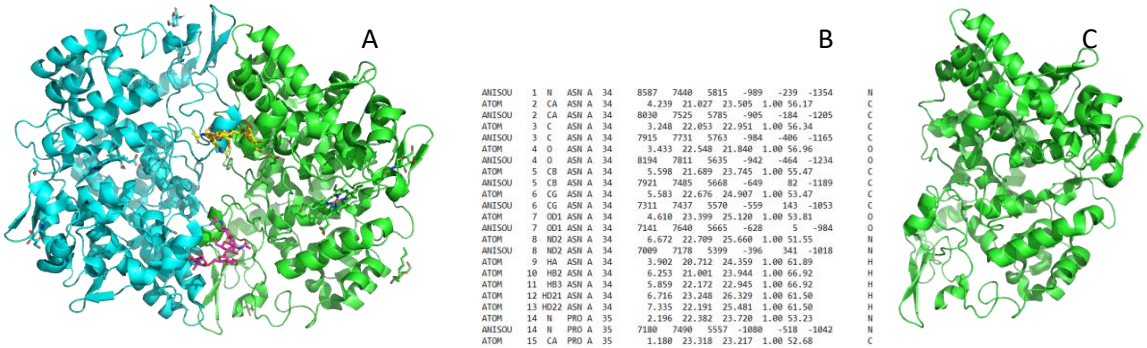

Figure 1 Optimization of the 5IKQ Protein Structure of COX-2 by Information Debugging for Molecular Docking. Note. 3D structure of the informationally complete 5IKQ molecule (A). Structural data will be deleted from the modified protein using Windows Notepad for optimization (C). Chain A of the protein as a result of protein model purification (B).

Using AutoDockTools software (Morris, G., Huey, R., Lindstrom, G., Sanner, M., Belew, R., Goodsell, D., & Olson, 2009) and with the protein prepared, we proceeded to the changing of the file format from .pdb to.

pdbqt, to the incorporation of charges. The optimization of the molecule so that the program could perform the protein-ligand interaction (Figure 3).

The Virtual Screening technique was used for the process of interaction between the 5IKQ protein and the 50 ligands (Chen et al., 2022). The virtual environment of the free access program Virtual Box version 6.1.34 (Opened Hand Ltd, 2009) was used in this process, simulating a Linux 64-bit version operating system, providing a virtual environment that is compatible with the Auto Dock Vina program (Morris, G., Huey, R., Lindstrom, G., Sanner, M., Belew, R., Goodsell, D., & Olson, 2009), which was used for molecular Docking in the Virtual Screening.

The protein and ligands were later copied to an external USB drive, specifically to a folder that was entered into the VirtualBox (Opened Hand Ltd, 2009) in which the Auto Dock Vina program was previously integrated (Morris, G., Huey, R., Lindstrom, G., Sanner, M., Belew, R., Goodsell, D., & Olson, 2009). Then the activation code of the Vina program "VINAv1.0.sh" (Trott O. & Arthur J., 2010) was typed in using the key commands, the information generated after the Virtual Screening processes was saved into the same USB drive, and the protein and ligand folders were selected.

Figure 2 shows a configuration file opened at the end of this process. The data of the active site of the 5IKQ protein, which was 2-[(2,6-dichloro-3-methyl-phenyl) amino] benzoic acid, was incorporated under the JMS identification in the .pdb file prior to the protein modifications.

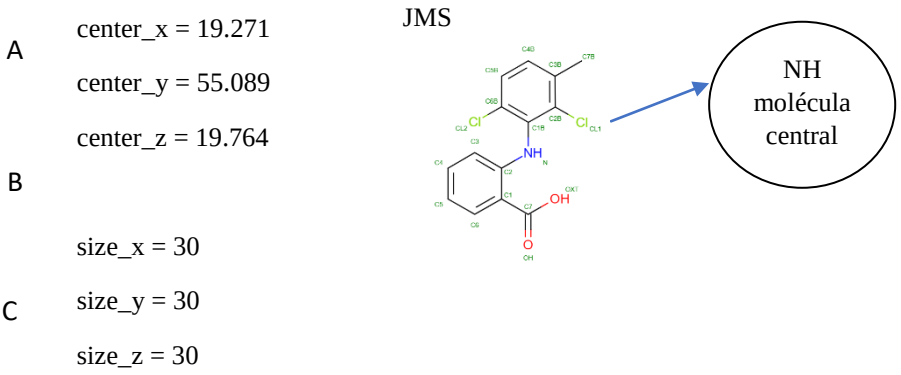

Figure 2. 5IKQ Protein Active Site Configurations file for Virtual Screening.

The file contains the protein active site information based on the central molecule of the JMS ligand. Three-dimensional representation of the central position of the ligand in the pdb of the COX-2 protein (A). The number of molecules that make up the ligand (B). The number of analyses suggested by Vina (C) (Trott O. & Arthur J., 2010).

The central carbon was placed in the reference ligand, and the information was extracted in the configuration file. Each process performed was summarized and schematized in Figure 3.

An HP Notebook model laptop with an x64 based PC system and an Intel(R) Core (TM) i5-5200U CPU @ 2.20GHz, 2201 Mhz, two central processors, four logical processors with an installed physical memory (RAM) 4.00 GB was used in the Virtual Screening process (Chen et al., 2022). To obtain the experimental results, the processing capacity was limited, and the waiting time was increased by 15 hours.

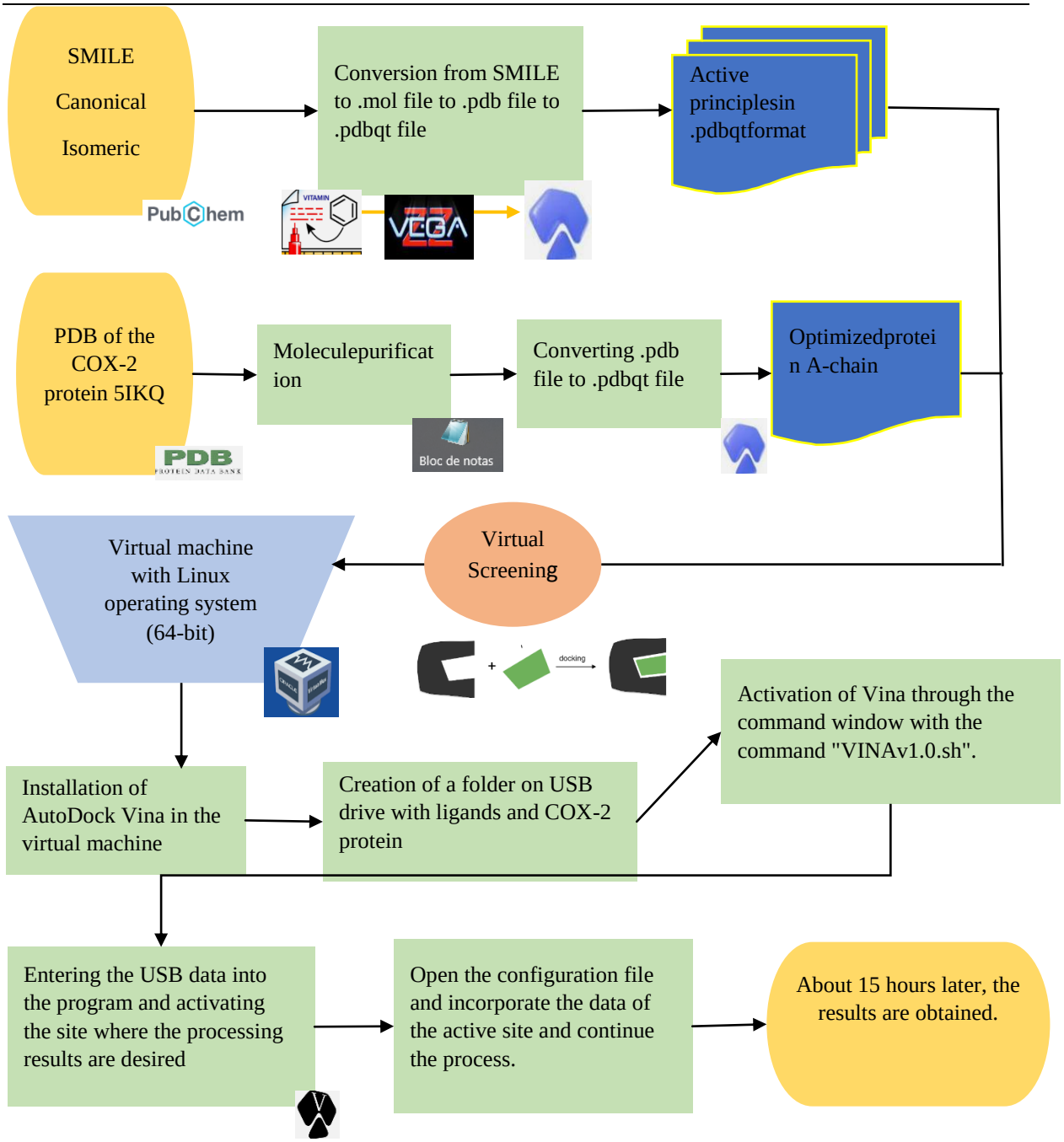

Figure 3. Molecular Dicking Procedure in Virtual Screening. Authors' elaboration

Results

Analysis of ligand-receptor interactions after Virtual Screening of the best molecular interactions.

As shown in Figure 4, image A, it was found that in the diagram of ligand interactions with COX-2 protein, Quercetin a Pentahydroxyflavone, with the presence of hydroxyl groups at positions 3, 3'-, 4'-, 4'-, 5- and 7, interact with the amino acids (aa) of the active site of the COX-2 protein. For this purpose, SER-A:353, VAL-A:523, and LEU-A:352 with π-sigma type bonds intervened in the interaction with the phenyl functional group and Benzopyran for LEU-A:352.

On the other hand, VAL-A:523 and SER-A:353 produced interactions with Benzopyran, which, due to its aromatic ring characteristics, promote a region of abundant electrons that enhance the interaction forces.

π-alkyl type interactions between VAL-A:349 and the aromatic structure of the phenyl functional group maintained a weak and unstable bond.

TYR-A:385 presented a negative interaction that did not produce favorable receptor activity, while HIS-A:90 had an interaction with the Hydroxyl in the Benzopyran, which promoted a hydrogen bridge. It generates excellent stability due to the interaction strength that establishes this type of bridge, making it the interaction that best suits the coupling.

Concerning Figure 4, image B, a two-dimensional representation of the interactions between the ligand Squalene and Triterpene with six double bonds in positions 2, 6, 10, 14, 18, and 22 of its chain structure, is observed. After the molecular coupling process, it acquired a semi-aromatic conformation and, therefore, interaction with multiple aa with π-alkyl type bonds through an interaction of a cloud of electrons that overlaps in an aromatic group of alkyl-type electrons.

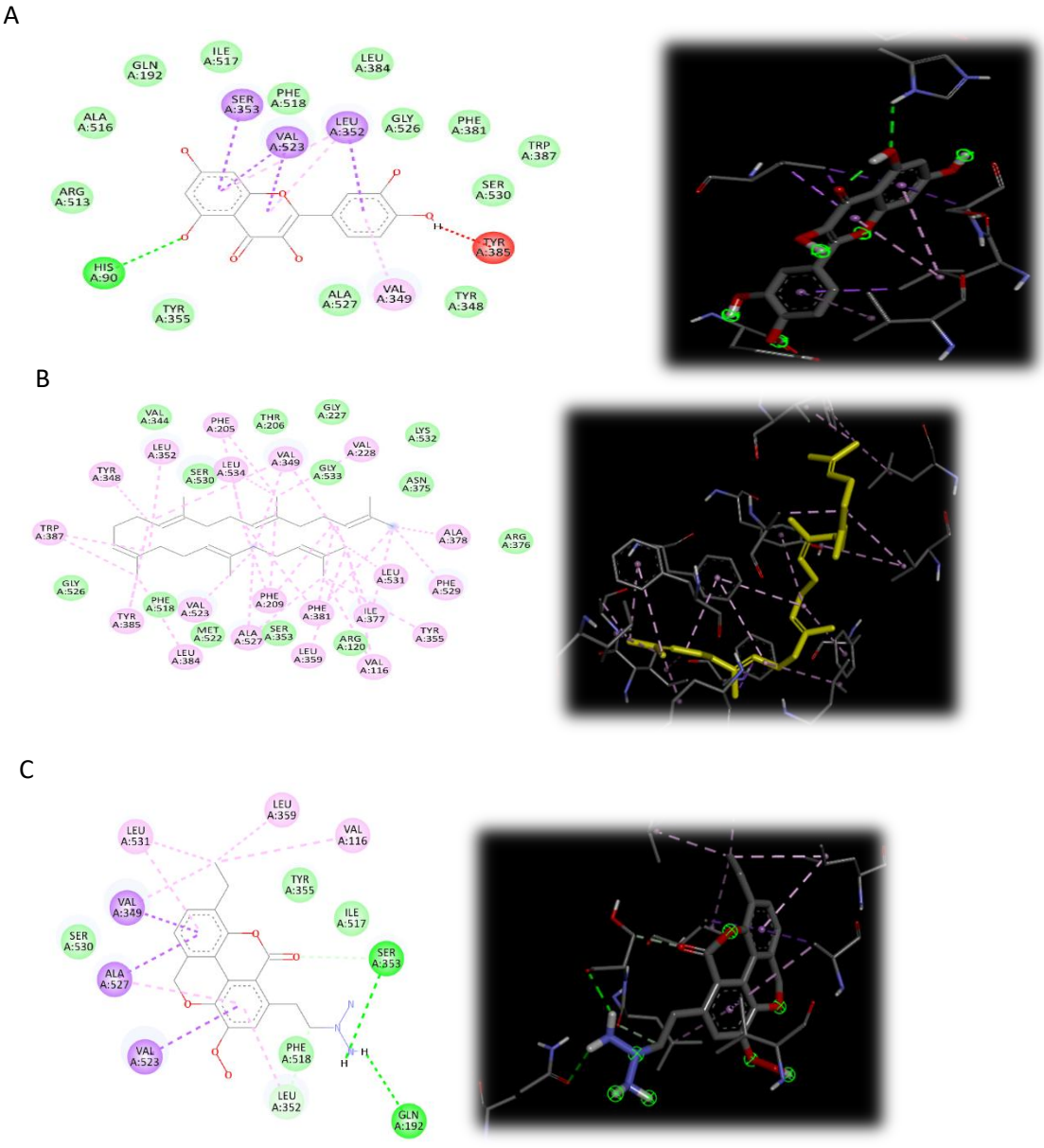

Figure 4. Molecular Docking Diagram of Bioactive Compounds to the central target of COX-2 Protein. Note: 2D interaction diagram of COX-2 protein with Quercetin (A) Squalene (B) Tapsine (C).

Finally, a 2D representation of the interactions is in Figure 4. Image C, there is the ligand Tapsine, where multiple π-sigma type interactions and π-alkyl type bonds were observed, which presented an interaction with alkyl type aromatic groups, for SER-A:353, GLN-A:192 a hydrogen bridges type interaction was observed which represented the interaction of higher bond strength and therefore higher stability.

The affinity of the active principles in the active site of the COX-2 protein

Fifty active principles of botanical species with wide distribution in Ecuador were used in the experiment.

The results obtained after the molecular coupling process range from -0.4 to -8.6 kcal/mol, from which the best-ranged interaction results presented in Table 3 were taken. The values provided after Virtual Screening were representative, more strongly as the value is more damaging, indicating higher affinity. In this case, the range was -8.6 kcal/mol, but the range can get up to -20 kcal/mol.

Table 3 Molecular Docking Results of the Best Active Ingredients on the COX-2 Protein Core Target

Scientific Name	Active Principle	Binding energy/kcal-mol-1	Binding site
Rivea corymbose (L.) Hallier f.	Quercetin	-8.6	HIS-A:90 SERA:353 VAL-A:523 LEU-A:352 VAL-A:349 TYR-A:385
Marsdenia condurango Rchb. f. Bark	Squalene	-8.4	TRP-A:387 TYR-A:348 LEU-A:352 LEU-A:534 PHE-A:205 VAL-A:349 VAL-A:228 ALA-A:378 TYR-A:385 LEU-A:384
Uncaria tomentosa (Will.) DC	Tapsine	-8.3	VAL-A:349 ALA-A:527 VAL-A:523 LEU-A:357 GLN-A:192 SER-A:353 VAL-A:116

Discussion

Bioinformatics tools are crucial for screening large amounts of information on potential therapeutic candidates (Abd-Elsalam, 2003; Bonsall et al., 2016) due to the silicic prediction in the study of protein-ligand affinities (Roskoski, 2022). These resources allow the comparative Analysis of diverse chemical compounds with broad origins. Therefore, it is becoming increasingly essential to incorporate silicic studies in experimental laboratory settings (Deftereos et al., 2011).

Table 3 presents the maximum values after the virtual screening performed on the active site of the COX-2 protein with results of an energetic range in Quercetin with -8.6 kcal/mol, in Squalene with -8.4 kcal/mol and Tapsine with -8.3 kcal/mol. Since the most negative values indicate a favorable interaction (Park et al., 2006), the results indicate a possible inhibitory capacity of the enzymatic activity of COX-2 protein (Lopez & Ballaz, 2020; Stachowicz, 2021). The values resemble similar experiments in which the energetic ranges were from -7.8 to -10.6 kcal/mol in Docking with fluorocurcumin analogs (Kothari et al., 2012; Mazard et al., 2016; Stachowicz, 2021). Thus, from a theoretical point of view, the possibility of establishing possible coupling mechanisms at the cellular level increases as a proposal to establish possible theoretical models that can then be tested through pharmacological kinetics at the metabolic level (Jade et al., 2020; Park et al., 2006; Sim et al., 2012).

Conclusions

The COX-2 inhibitory activity was evaluated through the Analysis of 50 active principles producing interaction results between the energetic ranges of -0.4 and -8.6 kcal/mol, allowing a better molecular coupling and stability in three possible inhibitors, Quercetin -8.6 kcal/mol (*Rivea corymbosa*), Squalene -8.4 kcal/mol (*Marsdenia condurango)* and Tapsine -8.3 kcal/mol (*Uncaria tomentosa*).

Through the molecular coupling technique, the study pointed out the theoretical pharmacological potential of the active principles present in botanical species of Ecuadorian origin in discarding compounds with low therapeutic potential. However, it is essential to include studies of the Quantitative Structure-Activity Relationships (QSAR) type and in vitro studies to verify what has been modeled theoretically at both experimental and metabolic levels.

References

[1]. Abd-Elsalam, K. A. (2003). Bioinformatic tools and guideline for PCR primer design. *African Journal of Biotechnology*, *2*(5), 91–95. https://doi.org/10.4314/ajb.v2i5.14794

[2]. Bailon-Moscoso, N., Romero-Benavides, J. C., Tinitana-Imaicela, F., & Ostrosky-Wegman, P. (2015). Medicinal plants of Ecuador: a review of plants with anticancer potential and their chemical composition. *Medicinal Chemistry Research 2015 24:6*, *24*(6), 2283–2296. https://doi.org/10.1007/S00044-015-1335-7

[3]. Bermúdez Arias, M. Á. (2017). *Mecanismo de activación de monocitos humanos por derivados oxidados del ácido araquidónico*. https://digital.csic.es/handle/10261/158298

[4]. Boltzmann, E. P., Atmospheric, W., & Energy, T. (2013). Fundamental Physical Constants. *Physics Today*. https://doi.org/10.1063/PT.4.0095

[5]. Bonsall, D., Gregory, W. F., Ip, C. L. C., Donfield, S., Iles, J., Ansari, M. A., Piazza, P., Trebes, A., Brown, A., Frater, J., Pybus, O. G., Goulder, P., Klenerman, P., Bowden, R., Gomperts, E. D., Barnes, E., Kapoor, A., Sharp, C. P., & Simmonds, P. (2016). Evaluation of Viremia Frequencies of a Novel Human Pegivirus by Using Bioinformatic Screening and PCR. *Emerging Infectious Diseases*, *22*(4), 671. https://doi.org/10.3201/EID2204.151812

[6]. Chahal, V., Nirwan, S., Pathak, M., & Kakkar, R. (2020). Identification of potent human carbonic anhydrase IX inhibitors: a combination of pharmacophore modeling, 3D-QSAR, virtual screening and molecular dynamics simulations. *Journal of Biomolecular Structure and Dynamics*, *40*(10), 4516–4531. https://doi.org/10.1080/07391102.2020.1860132

[7]. Chen B, Wild D, G. R. (2009). PubChem as a source of polypharmacology. *J Chem Inf Model*, *49*(9), 2044–2055. https://pubchem.ncbi.nlm.nih.gov//docs/about

[8]. Chen, X. Z., Yu, X. Y., Dai, C., Huang, Q. Y., Shen, Y., Wang, J., Hu, Y., & Lin, Z. H. (2022). Identification of potent CypD inhibitors via pharmacophore based virtual screening, docking and molecular dynamics simulation. *Journal of Molecular Structure*, *1247*, 131355. https://doi.org/10.1016/J.MOLSTRUC.2021.131355

[9]. Danielsen, F., Burgess, N. D., & Balmford, A. (2005). Monitoring matters: Examining the potential of locally-based approaches. *Biodiversity and Conservation*, *14*(11), 2507–2542. https://doi.org/10.1007/S10531-005-8375-0

[10]. Deftereos, S. N., Andronis, C., Friedla, E. J., Persidis, A., & Persidis, A. (2011). Drug repurposing and adverse event prediction using high-throughput literature analysis. En *Wiley Interdisciplinary Reviews: Systems Biology and Medicine* (Vol. 3, Número 3, pp. 323–334). https://doi.org/10.1002/wsbm.147

[11]. Egwolf, B., & Gumawid, J. M. A. (2020). Molecular docking of modified ipalbidine ligands into human cyclooxygenase-2 protein crystal structures. *Journal of Physics: Conference Series*, *1529*(3).

[12]. Firdous, S. M., & Sautya, D. (2018). Medicinal plants with wound healing potential. *Bangladesh Journal of Pharmacology*, *13*(1), 41–52. https://doi.org/10.3329/BJP.V13I1.32646

[13]. Fujikura, K., Ingelman-Sundberg, M., & Lauschke, V. M. (2015). Genetic variation in the human cytochrome P450 supergene family. *Pharmacogenetics and Genomics*, *25*(12), 584–594. https://doi.org/10.1097/FPC.0000000000000172

[14]. Ihlenfeldt W, Bolton E, B. S. (2009). The PubChem chemical structure sketcher. *J Cheminform*, *1*(1), 20. https://pubchem.ncbi.nlm.nih.gov//docs/about

[15]. Jade, D. D., Pandey, R., Kumar, R., & Gupta, D. (2020). Ligand-based pharmacophore modeling of TNF-α to design novel inhibitors using virtual screening and molecular dynamics. *https://doi.org/10.1080/07391102.2020.1831962*, *40*(4), 1702–1718. https://doi.org/10.1080/07391102.2020.1831962

[16]. Kedika, R. R., Souza, R. F., & Spechler, S. J. (2009). Potential Anti-inflammatory Effects of Proton Pump Inhibitors: A Review and Discussion of the Clinical Implications. *Digestive Diseases and Sciences 2009 54:11*, *54*(11), 2312–2317. https://doi.org/10.1007/S10620-009-0951-9

[17]. Kothari, R., Pathak, V. V., Kumar, V., & Singh, D. P. (2012). Experimental study for growth potential of unicellular alga Chlorella pyrenoidosa on dairy waste water: An integrated approach for treatment and biofuel production. *Bioresource Technology*, *116*, 466–470. https://doi.org/10.1016/J.BIORTECH.2012.03.121

[18]. Laskowski, R. A., MacArthur, M. W., Moss, D. S. & Thornton, J. M. (1993). *PROCHECK: a program to check the stereochemical quality of protein structures.* https://scholar.google.com/scholar?q=Laskowski%2C%20R.%20A.%2C%20MacArthur%2C%20M.%20W.%2C%20Moss%2C%20D.%20S.%20%26%2338%3B%20Thornton%2C%20J.%20M.%20%281993%29.%20PROCHECK%3A%20a%20program%20to%20check%20the%20stereochemical%20quality%20of%20protein%20s. https://onlinelibrary.wiley.com/iucr/itc/Fb/ch21o3v0001/sec21o3o3o1/

[19]. López, D. E., & Ballaz, S. J. (2020). The Role of Brain Cyclooxygenase-2 (Cox-2) Beyond Neuroinflammation: Neuronal Homeostasis in Memory and Anxiety. *Molecular Neurobiology 2020 57:12*, *57*(12), 5167–5176. https://doi.org/10.1007/S12035-020-02087-X

[20]. María, R., Shirley, M., Xavier, C., Jaime, S., David, V., Rosa, S., & Jodie, D. (2018). Preliminary phytochemical screening, total phenolic content and antibacterial activity of thirteen native species from Guayas province Ecuador. *Journal of King Saud University - Science*, *30*(4), 500–505. https://doi.org/10.1016/J.JKSUS.2017.03.009

[21]. Mazard, S., Penesyan, A., Ostrowski, M., Paulsen, I., & Egan, S. (2016). Tiny Microbes with a Big Impact: The Role of Cyanobacteria and Their Metabolites in Shaping Our Future. *Marine Drugs*, *14*(5), 97. https://doi.org/10.3390/md14050097

[22]. Morris, G., Huey, R., Lindstrom, G., Sanner, M., Belew, R., Goodsell, D., & Olson, A. (2009). AutoDockTools (N^{o} de versión 1.5.6 Sep_17_14). Windows. *The Scripps Research Institute*. https://autodock.scripps.edu/

[23]. Nag., Dhull, N., & Gupta, A. (2022). Evaluation of tea (Camellia sinensis L.) phytochemicals as multi-disease modulators, a multidimensional in Silico strategy with the combinations of network pharmacology, pharmacophore analysis, statistics and molecular docking. *Molecular diversity*, 1–23.

[24]. OpenedHand Ltd. (2009). *Oracle R VM VirtualBox*. versión 7.0.4. https://www.virtualbox.org/wiki/Changelog-7.0#v4

[25]. Page, C. P., & Spina, D. (2011). Phosphodiesterase inhibitors in the treatment of inflammatory diseases. *Handbook of Experimental Pharmacology*, *204*, 391–414. https://doi.org/10.1007/978-3-642-17969-3_17/COVER

[26]. Park, J. Y., Pillinger, M. H., & Abramson, S. B. (2006). Prostaglandin E2 synthesis and secretion: The role of PGE2 synthases. *Clinical Immunology*, *119*(3), 229–240. https://doi.org/10.1016/J.CLIM.2006.01.016

[27]. Pedretti, A., & Vistoli, G. (2006). *Vega ZZ N^{o} de versión: 3.2.2.20*. Milán, Italia: Università degli Studi di Milano. https://www.ddl.unimi.it/cms/index.php?Software_projects:VEGA_ZZ

[28]. Roskoski, R. (2022). Janus kinase (JAK) inhibitors in the treatment of neoplastic and inflammatory disorders. *Pharmacological Research*, *183*, 106362. https://doi.org/10.1016/J.PHRS.2022.106362

[29]. Sánchez-Mendoza, M. A., Martínez-Ayala, S. O., Hernández-Hernández, J. A., Zúñiga-Sosa, L., Pastelín-Hernández, G., & Escalante-Acosta, B. A. (2003). Participación del óxido nítrico y los metabolitos del ácido araquidónico vía citocromo P450 en la regulación de la presión arterial. *Archivos de Cardiología de México*, *73*(2), 98–104.

[30]. Sim, S. C., Daly, A. K., & Gaedigk, A. (2012). CYP2D6 update: Revised nomenclature for CYP2D7/2D6 hybrid genes. En *Pharmacogenetics and Genomics* (Vol. 22, Número 9, pp. 692–694). https://doi.org/10.1097/FPC.0b013e3283546d3c

[31]. Sobolev, O. V., Afonine, P. V., Moriarty, N. W., Hekkelman, M. L., Joosten, R. P., Perrakis, A., & Adams, P. D. (2020). A Global Ramachandran Score Identifies Protein Structures with Unlikely Stereochemistry. *Structure*, *28*(11), 1249-1258.e2. https://doi.org/10.1016/j.str.2020.08.005

[32]. Stachowicz, K. (2021). Deciphering the mechanisms of regulation of an excitatory synapse via cyclooxygenase-2. A review. *Biochemical Pharmacology*, *192*, 114729. https://doi.org/10.1016/J.BCP.2021.114729

[33]. Trott O. and Arthur J. (2010). AutoDock Vina: improving the speed and accuracy of docking with a new scoring function, efficient optimization, and multithreading. *Journal of computational chemistry*, *31*(2), 455–461.

[34]. Zhang, Q., Ren, Y., Mo, Y., Guo, P., Liao, P., Luo, Y., Mu, J., Chen, Z., Zhang, Y., Li, Y., Yang, L., Liao, D., Fu, J., Shen, J., Huang, W., Xu, X., Guo, Y., Mei, L., Zuo, Y., … Jiang, R. (2022). Inhibiting Hv1 channel in peripheral sensory neurons attenuates chronic inflammatory pain and opioid side effects. *Cell Research*, *32*(5), 461–476. https://doi.org/10.1038/s41422-022-00616-y